Estimation of Spalling Stress in Thermal Barrier Coatings Using Hard Synchrotron X-Rays*

Kenji SUZUKI**, Keisuke TANAKA*** and Yoshiaki AKINIWA***

It is possible to measure nondestructively the residual stress in the interior of the top coating in the thermal barrier coating (TBC) using hard synchrotron X-rays, which have a large penetration depth and high brightness. A new hybrid method is proposed to estimate the distribution of the spalling stress in the top coating by combining the synchrotron data with the stress data measured by the conventional X-ray method utilizing a Cr-Kα radiation. The new hybrid method was applied to estimate the distribution of the spalling stress in the top coating of TBC which had a zirconia top coating with a thickness of 0.24 mm and a NiCoCrAlY bond coating with a thickness of 0.2 mm. The residual stress, $\sigma_{11}-\sigma_{33}$, within the top coating was determined by synchrotron X-rays of 73 keV energy level, where σ_{33} was the stress perpendicular to the surface and σ_{11} was an in-plane stress. The distribution of residual in-plane stresses, σ_{11} and σ_{22}, in the top and the bond coating was determined with the conventional X-ray method by repeating the measurement after successive removal of the surface layer. From the data obtained by synchrotron and conventional X-rays, the distribution of stress component, σ_{33}, responsible for spalling was determined. The estimated value of the spalling stress was very small beneath the surface and increased to about 75 MPa near the interface between the top and the bond coating.

Key Words: Residual Stress, Experimental Stress Analysis, Nondestructive Inspection, Delamination, Wear, Thermal Barrier Coating, X-Ray Stress Measurement

1. Introduction

A thermal barrier coating (TBC) is a key technology of gas turbine engines. The TBC consists of a top coating plasma-sprayed with zirconia and a bond coating plasma-sprayed with MCrAlY. It is the most important to prevent the TBC from a spallation of the top coating. There are many factors of the spallation of the TBC, for example, a thermal stress due to a difference in thermal expansion between the top and the bond coating, thermally growth oxide and a residual stress caused by the interface roughness. Estimation of internal stresses in TBCs is indispensable for improving the TBC technology. The interface asperity between the top and the bond coating causes spallation of the TBC[1),(2)]. The spallation of TBCs has been analyzed mainly by a finite element method, and then the relation between the interface asperity and the spalling stress has been investigated[3),(4)]. However, TBCs have the complicated mechanical behaviour with lamella structure[5)]. It is very difficult to analyze the spalling stress by taking account of the mechanical properties of TBCs. On the other hand, the residual stresses in TBCs were measured experimentally, such as photo-stimulated luminescence spectroscopy[6),(7)].

The residual stress beneath the surface of the top coating can be measured by the conventional X-ray method[8)]. Because high energy X-rays have deep penetration depth, internal stresses of the bond coating can be measured nondestructively through the top coating using the synchrotron radiation source[9)]. It is very useful to apply both of low and high energy X-rays for the estimation of the spalling stress in TBCs.

In this study, a new method is proposed to estimate the spalling stress in top coatings by combining the stresses measured by low and high energy X-rays.

* Received 11th December, 2003 (No. 03-4198)

** Department of Technology and Living Sciences, Niigata University, 8050 Igarashi-2no-cho, Niigata 950–2181, Japan. E-mail: suzuki@ed.niigata-u.ac.jp

*** Department of Mechanical Engineering, Nagoya University, Furoh-cho, Chikusa-ku, Nagoya, Aichi 464–8603, Japan

2. Analysis of Spalling Stress

The X-ray penetration depth becomes large with the increase in the X-ray energy. The change in the X-ray penetration depth with the increase in the X-ray energy is shown in Fig. 1. The effective penetration depth is calculated for the 333 diffraction of the zirconia top coating in the condition of the side-inclination configuration. As shown in the figure, the penetration depth for low energy X-rays is small, and the measured stress is the in-plane stress. For high energy X-rays from a synchrotron radiation source, the penetration depth becomes very large, for instance, the penetration depth for 72 keV X-rays is over 50 μm. Hence, the stress measured with high energy X-rays includes not only the in-plane stress but also the out-of-plane stress.

In this section, a new analysis on a spalling stress using a low and a high energy X-ray is described. The coordinate system and the principal stresses used are defined as shown in Fig. 2, where σ_X is a stress measured by the X-ray method. ψ is the angle between a normal to the specimen surface and a normal to the diffraction plane. The relation between the measured diffraction angle, 2θ, and the stresses is expressed as[10]

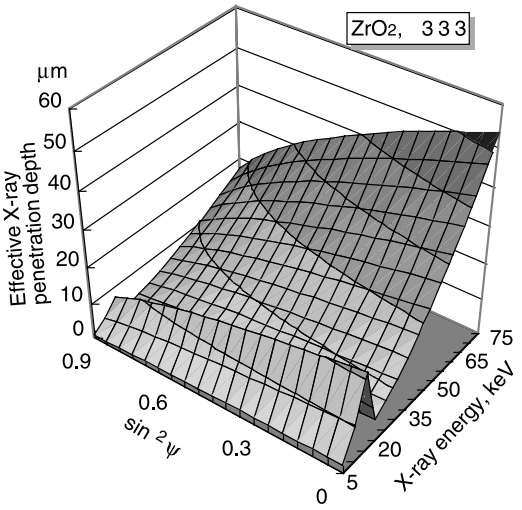

Fig. 1 X-ray penetration depth of TBC for high energy X-rays

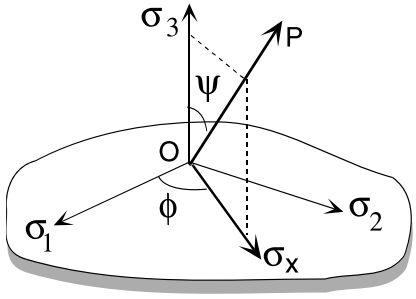

Fig. 2 Coordinate system for stress measurements

$$2\theta = 2\theta_0 - \frac{2(1+\nu_X)}{E_X}\tan\theta_0(\sigma_X - \sigma_3)\sin^2\psi - \frac{2}{E_X}\tan\theta_0\sigma_3 + \frac{2\nu_X}{E_X}\tan\theta_0(\sigma_1+\sigma_2) \quad (1)$$

where θ_0 is the diffraction angle for strain-free material, E_X and ν_X are the X-ray elastic Young's modulus and the Poisson's ratio, respectively. Assuming $\sigma_1 = \sigma_2 = \sigma_X$, Eq. (1) is rewritten as follows:

$$2\theta = 2\theta_0 - \frac{2(1+\nu_X)}{E_X}\tan\theta_0(\sigma_1 - \sigma_3)\sin^2\psi - \frac{2}{E_X}\tan\theta_0\sigma_3 + \frac{4\nu_X}{E_X}\tan\theta_0\sigma_1 \quad (2)$$

For low energy X-rays, the stress beneath the surface is measured, and the plane stress state, i.e. $\sigma_3 = 0$, can be assumed. We can obtain the following equation by partial differential of Eq. (2) by $\sin^2\psi$.

$$\frac{\partial 2\theta}{\partial \sin^2\psi} = -\frac{2(1+\nu_X)}{E_X}\tan\theta_0\sigma_1 \quad (3)$$

Hence, the in-plane stress, σ_1, can be determined from the gradient of the $2\theta - \sin^2\psi$ diagram. The X-ray stress, $\sigma_{x\text{-ray}}$ is regarded as the in-plane stress.

$$\sigma_{x\text{-ray}} = \sigma_1 \quad (4)$$

When the stress is measured by high energry X-rays from a synchrotron source, the stress state is no longer the plane stress, because of its large penetration depth and the spalling stress existing near the interface between the top and the bond coating. The gradient of the $2\theta - \sin^2\psi$ diagram measured with high energy X-rays is

$$\frac{\partial 2\theta}{\partial \sin^2\psi} = -\frac{2(1+\nu_X)}{E_X}\tan\theta_0(\sigma_1 - \sigma_3) \quad (5)$$

Thus, the stress measured by high energry X-rays, σ_{syn}, is given by

$$\sigma_{syn} = \sigma_1 - \sigma_3 \quad (6)$$

From the relation between Eqs. (4) and (6), the spalling stress, σ_3, is obtained.

$$\sigma_3 = \sigma_{x\text{-ray}} - \sigma_{syn} \quad (7)$$

The method to estimate the spalling stress, σ_3, by combining σ_1 measured by low energy X-rays and $\sigma_1 - \sigma_3$ measured by high energy X-rays, is named the hybrid method in the present study. In the following analysis, the change in the X-ray penetration depth with the change in ψ angle, however, is not considered for the sake of simplicity.

3. Experiments

3.1 Materials and specimens

The bond coating was made of NiCoCrAlY which was low pressure plasma-sprayed on the substrate of Ni base super-alloy with the thickness of 2 mm. The thickness of the bond coating was 0.2 mm. The top coating of zirconia with 8 wt% was made by air plasma-spraying

on the bond coating. The thickness of the top coating was 0.2 mm. After heating the TBCs in vacuum, the specimens were cut into the dimensions of 8 mm in width and 60 mm in length.

The mechanical Young's modulus of the top coating was measured by the tension test of the free-standing top coating, which was removed from the TBC specimen by electropolishing. The detail of the tension test of the TBC specimen is described in our previous study[8]. The Young's modulus was 87.0 GPa and the tensile strength was 7.88 MPa. To measure the mechanical Young's modulus of the bond coating, the free-standing bond coating specimen was prepared. The free-standing specimen with the thickness of 1 mm was made by grinding the substrate. The tension test of the free-standing bond coating specimen was performed with the tension tester (AUTOGRAPH) and the strain was measured with a strain gauge. For the bond coating, the Young's modulus and the Poisson's ratio were 158 GPa and 0.27, respectively.

3.2 X-ray conditions

The in-plane stresses of the top and bond coatings were measured by the conventional X-ray method. The diffractions used were ZrO_2 133+331 for the top coatings and Ni_3Al 220 for the bond coating by the Cr-Kα characteristic X-rays. The conditions for X-ray stress measurements are shown in Table 1. The X-ray optics is the parallel beam method, and the $\sin^2\psi$ method and the iso-inclination configuration (Ω-goniometer) were used for the X-ray stress measurements. The value of the X-ray elastic constant of the top coating, which was obtained from our previous study[8], was used in stress calculation. The value of the X-ray elastic constant of the top coating was independent of coating conditions. The mechanical elastic constants, on the other hand, depend on the top coating structure such as pores, lamella structure and cracks. The X-ray elastic constant of the top coating was obtained by the experiment using the free-standing bond coating specimen.

The experiment by the high energy X-ray was performed with the 4-circle goniometer at the beam line BL02B1 in the Japan synchrotron research institute, SPring-8. The conditions for stress measurements by synchrotron radiations were shown in Table 2. For the stress measurement of the top coating, the diffraction from ZrO_2 511+333 was used. For the stress measurement of the bond coating, the diffraction from Ni_3Al 311 was used. Each stress constant was calculated from X-ray elastic constant used for the above X-ray stress measurement. In measuring the residual stress, the specimens were set on the rotating table in order to assume the equi-biaxial stress state. The used method for the stress measurement was $\sin^2\psi$ method with the side-inclination configuration (Ψ-goniometer).

The X-ray wavelength was 73.23 keV, so that both

Table 1 X-ray conditions for stress measurement

	Top coating	Bond coating
Crystal	ZrO_2	Ni_3Al
Diffraction	133+331	2 2 0
$2\theta_0$	153.82 deg	129.35 deg
Radiations	Cr-Kα	Cr-Kα
Tube voltage	40 kV	40 kV
Tube current	30 mA	30 mA
Filter	V	V
Scanning	0.1°/step	0.05°/step
Divergent angle	0.64°	0.64°
Irradiated area	4×8 mm^2	4×8 mm^2
$\sin^2\psi = 0 \sim 0.6$	0.05 step	0.1 step
Stress constant	−229MPa/deg	−728MPa/deg

Table 2 Conditions for stress measurement with synchrotron X-rays

Wavelength	0.016932 nm (73.23 keV)	
Slit size, $(w \times h)$	2×0.5 mm^2	
Method	Side inclination configuration	
	Top coating	Bond coating
Crystal	ZrO_2	Ni_3Al
Diffraction	511+ 333	311
$2\theta_0$ (deg)	9.8090	9.0135
Stress constant (MPa/deg)	−11492	−19486
$\sin^2\psi$	$0 \sim 0.7$ (step 0.05)	

diffraction angles are lower than 10 deg. Therefore, the high accurate measurement is required. The long soller slit was attached front the scintillation counter in order to reduce the broadening of diffraction profiles. The sampling time was determined enough to become the peak hight over 3 000 counts.

4. Results and Discussion

4.1 Distribution of residual stress measured by laboratry X-rays

To obtain the distribution of the residual stress in the direction of depth, the stress measurement with low energy X-rays was repeated successively after removal on the TBC surface with diamond slurry. Figure 3 (a) shows the distribution of the residual stress of the in-plane stress. As shown the figure, the residual stress of the top coating was a small tension near the coating surface. This is caused by a release of a stress due to the surface roughness and micro-cracks. With the increase in the depth, the residual stress increases to about 50 MPa, and becomes constant. Approaching the interface between the top and the bond coating, the residual stress of the top coating increases, and then decreases.

The residual stress of the bond coating is large compression near the interface between the top and the bond coating, and it increases with the increase in the depth. The residual stresses in the bond coating changes from

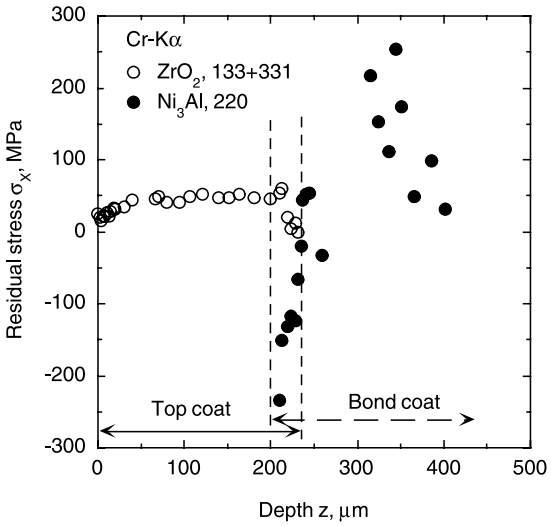

(a) Residual stress distribution

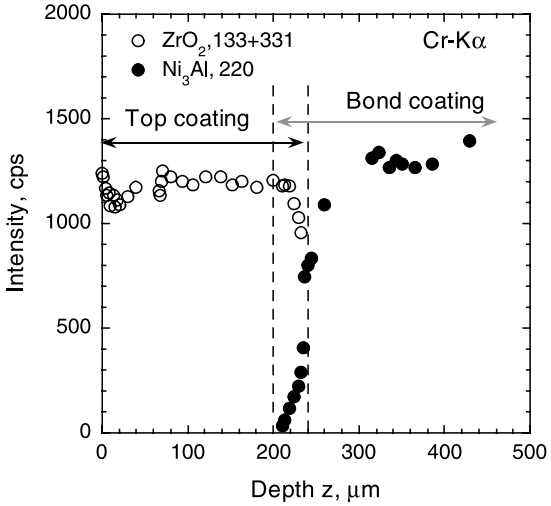

(b) Intensity distribution

Fig. 3 Change in residual stress and X-ray intensity in the direction of depth

large tension to zero close to the interface between the bond coating and the substrate.

Figure 3 (b) shows the change in the diffraction intensities with the removed depth. The asperity of the interface between the top and the bond coating is expressed by the difference in the diffraction intensities between the top and the bond coating. As shown in the figure, the X-ray intensity from the zirconia top coating strated decreasing from the depth of 200 μm and went out at the depth of about 240 μm. The asperity of the interface is therefore about 40 μm.

4.2 Residual stress measured by synchrotron

The diffraction profiles, which were obtained by high energy X-rays from synchrotron source, are shown in Fig. 4. In the figure, T_c is the thickness of the top coating, the specimen for $T_c = 240\,\mu m$ is as coated. The figure also shows the diffraction profiles for the specimens with several kinds of the thickness of the top coating. The thicknesses of the top coating were completed by buffing with diamond slurry with a great case not to introduce additional residual stresses. In addition of the diffraction curve for the specimen as top coated ($T_c = 240\,\mu m$), diffraction curves for the others specimens were also shown in Fig. 4. As shown in the figure, it is noted that the diffraction of the bond coating can be measured through the top coating using high energy X-rays. The diffraction intensities from the bond coating became strong with the decrease in the thickness of the top coating, T_c. Particularly, the 311 diffraction from Ni_3Al has the strong intensity, and it is suitable for the stress measurement. Although the 422 diffraction from ZrO_2 has the strong intensity, there is the 222 diffraction from Ni_3Al near the right side of it. Therefore, the 511+333 diffractions from ZrO_2 were used for the stress measurement of the top coating. The X-ray with energy above 73 keV has deeper penetration depth, but the diffraction angle, 2θ, becomes too low to measure the stress. As a result, the X-ray energy of about 73 keV is the most suitable energy level for the stress measurement of TBCs.

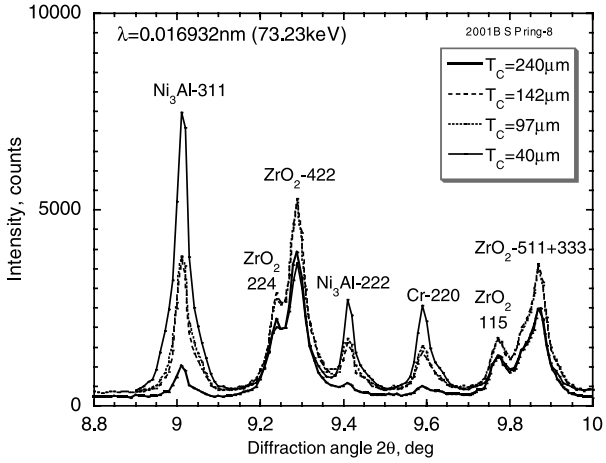

Fig. 4 Diffraction profiles of TBCs for several thicknesses by synchrotron X-rays

The thicknesses of the top coating, T_c, were 240 μm, 142 μm, 97 μm, 40 μm, and 0 μm. For these specimens, the residual stresses of the top and the bond coating were measured by synchrotron X-rays with the energry of 73.23 keV. The $2\theta - \sin^2\psi$ diagrams of the top and the bond coating are shown in Fig. 5 (a) and (b). Although there are the small deviations and waviness in the diagrams, the relations can be approximated by the straight lines. Each fitting line is indicated in the figures. The value of the stress was calculated from the gradient of the fitting line.

The obtained stress are shown in Table 3. As shown the table, the residual stress of the top coating as sprayed was small tensile, and the residual stress became small compressive with the decrease in the thickness of the top

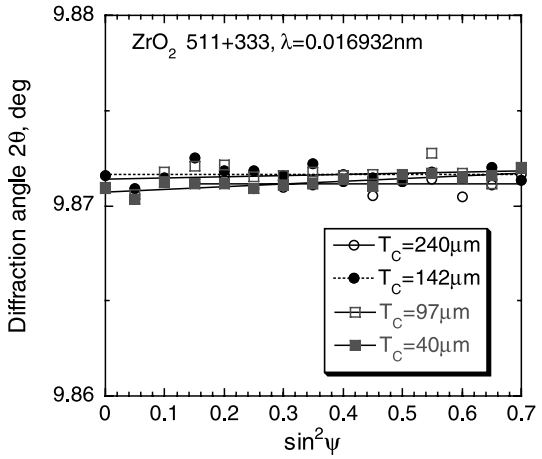

(a) Top coating

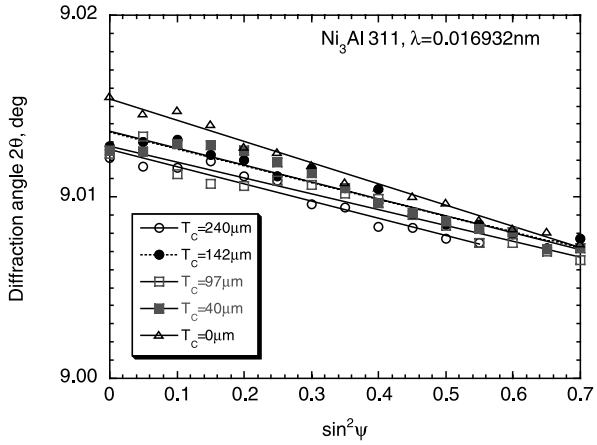

(b) Bond coating

Fig. 5 $2\theta - \sin^2\psi$ diagrams of TBC using synchrotron radiation

Table 3 Residual stresses measured by synchrotron

Thickness of top coating T_c	Residual stress σ_{syn} (MPa)	
	Top coating	Bond coating
240 μm	5.0	185
142 μm	1.6	183
97 μm	−7.4	175
40 μm	−15.6	178
0 μm	—	222

coating. It is noted that the tendancy for the residual stress of the top coating measured by high energy synchrotron X-rays is different from that by low energy X-rays with Cr-Kα shown in Fig. 3. This difference comes from that the stresses measured by the synchrotron X-rays include the stresses at the deep position from the surface due to its large penetration depth, while the stresses measured by the low energy X-rays are the in-plane stresses due to its small penetration depth.

4.3 Spalling stress in top coating

The spalling stress in the TBC is estimated by the hybrid method using Eq. (7). The results are shown in Fig. 6.

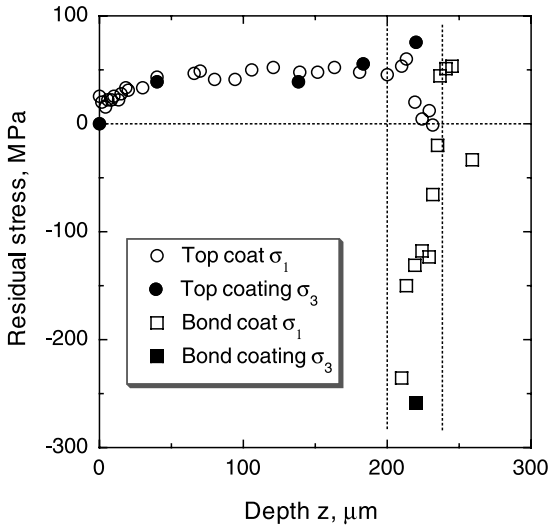

Fig. 6 Distribution of residual stress determined by the hybrid method

In the figure, the in-plane stresses, σ_1, are plotted at the removed depth. Each σ_3 is plotted at the depth of 40 μm from the removed surface, because the mean of the penetration depth from $\sin^2\psi = 0$ to 0.7 is 40 μm in the case of the synchrotron X-ray energy of 73.23 keV. However, σ_3 for the specimen of $T_c = 40\,\mu$m, is plotted at a half thickness, $T_c/2 = 20\,\mu$m, to take account of the remaining thickness of the top coating. The spalling stress, σ_3, for the bond coating was calculated from the mean of $\sigma_1 - \sigma_3$ for the bond coating and the mean of σ_1 from $z = 200\,\mu$m to 240 μm. And then, the spalling stress of the bond coating is plotted at $z = 220\,\mu$m which is the mean depth of the interface between the top and bond coating.

The spalling stress for the top coating is zero at the surface and has the constant value of about 40 MPa. And then, the spalling stress becomes large near the interface between the top and bond coating. The spallation of the top coating is controlled by the compressive in-plane stress and the spalling stress. As the in-plane stress, σ_1, is a tension as shown in the figure, the measured stress, σ_3, is not enough for the spallation. The magnitude of the spalling stress estimated by the hybrid method is reasonable as the TBC specimen after annealing. The interface between the top and the bond coating has the complex asperity, and the residual stress near the interface consists of the local phase stresses of the zirconia top coating and the bond coating. The stress measured by X-rays is the phase stress of zirconia, hence the out-of-plane stress of zirconia exists near the interface. The out-of-plane stress in the bond coating is compressive against the tensile stress in the top coating. The existence of the large spalling stresses near the interface corresponds to the thought that the spalling stress is caused by the asperity of the interface between the top and the bond coating[1),2)].

On the other hand, a spalling stress is strongly pro-

moted by thermally grown oxide[11),12)], it is useful to estimate a spalling stress by the hybrid method. The mechanism of spallation of the TBCs will be clarified by utilizing the high energy synchrotron X-rays as the experimental method for the starin analysis.

5. Conclusions

The TBC specimen plasma-spayed was prepared to have the zirconia top coating with the thickness of 0.2 mm and the NiCoCrAlY bond coating with the thickness of 0.2 mm. The distribution of the in-plane stress in the top coating was obtained by repeating the conventional X-ray stress measurement after successive removal. The residual stresses of the TBC specimens with several thicknesses were measured by synchrotron X-rays with the energry of 73.23 keV.

The obtained results are summarized as follows:

(1) The in-plane stress in the top coating was a small tension beneath the surface, and increased near the interface between the top and the bond coating. The in-plane stress in the bond coating was compressive near the interface with top coating. It changed from compression to tension with the distance from the interface.

(2) The residual stress in the bond coating could be measured through the top coating using high energry synchrotron X-rays. The diffraction from Ni_3Al 311 with 73 keV showed very strong intensity. The diffraction from ZrO_2 511+333 with the X-ray energy of 73.23 keV is suitable for the stress measurement of the top coating.

(3) The spalling stress in the TBC was estimated by combining low and high energry X-rays, and this method was named the hybrid method. The spalling stress in the top coating became 75 MPa near the interface between the top and the bond coating.

Acknowledgement

This work was supported financially by a grant-in-aid for science research from the Ministry of Education, Culture, Sports, Science and Technology of Japan (No. 13650078). The synchrotron radiation experiments were performed at SPring-8 with approval of the Japan Synchrotron Radiation Research Institute (Proposal No. 2001B-0063-Nd-np, 2002A-0116-ND1-np, and TU-3). The authors are obliged to Dr. N. Ikeda (JASRI), K. Nishio, H. Okado and M. Kawamura (Kawasaki Heavy Industries, Ltd.) for assistance of the experiments and helpful suggestions.

References

(1) Evans, A.G., Crumley, G.B. and Demaray, R.E., On the Mechanical Behavior of Brittle Coatings and Layers, Oxidation of Metals, Vol.20 (1983), pp.193–216.

(2) Bordeaux, F., Saint-Jacques, R.G., Moreau, C., Dallaire, S. and Lu, J., Thermal Shock Resistance of TiC Coatings Plasma Sprayed onto Macroroughened Substrates, Surf. Coat. Technol., Vol.53 (1992), pp.49–56.

(3) Ahrens, M., Vaßen, R. and Stöver, D., Stress Distributions in Plasma-Sprayed Thermal Barrier Coatings as a Function of Interface Roughness and Oxide Scale Thickness, Surf. Coat. Technol., Vol.161 (2002), pp.26–35.

(4) Hsueh, C.H. and Fuller, E.R., Jr., Residual Stresses in Thermal Barrier Coatings: Effects of Interface Asperity Curvature/Height and Oxide Thickness, Mater. Sci. and Eng., A, Vol.283 (2000), pp.46–55.

(5) Suzuki, K., Machiya, S., Tanaka, K. and Sakaida, Y., X-Ray Study on Deformation Characteristics of Thermal Barrier Coating Films, Trans. JSME, Ser. A, (in Japanese), Vol.67 (2001), pp.1325–1331.

(6) Sohn, Y.H., Vaidyanathan, K., Ronski, M., Jordan, E.H. and Gell, M., Thermal Cycling of EB-PVD/MCrAlY Thermal Barrier Coatings: II Evolution of Photo-Stimulated Luminescence, Surf. Coat. Technol., Vol.146–147 (2001), pp.102–109.

(7) Tolpygo, V.K., Clarke, D.R. and Murphy, K.S., Oxidation-Induced Failure of EB-PVD Thermal Barrier Coatings, Surf. Coat. Technol., Vol.146–147 (2001), pp.124–131.

(8) Suzuki, K., Machiya, S., Tanaka, K. and Sakaida, Y., X-Ray Elastic Constants and Residual Stress Distributions of Zirconia Thermal Barrier Coating, Trans. JSME, Ser. A, (in Japanese), Vol.67 (2001), pp.417–423.

(9) Suzuki, K., Tanaka, K., Akiniwa, Y., Kawamura, M., Nishio, K. and Okado, H., Measurements of Internal Stress in Bond Coating Using High Energy X-Rays from Synchrotron Radiation Source, J. Japan Soc. of Synch. Radiation Research, (in Japanese), Vol.15 (2002), pp.347–353.

(10) JSMS-SD1-00, Standard for X-Ray Stress Measurements — Ceramics —, (in Japanese), (2000), p.30, JSMS.

(11) Caliez, M., Feyel, F., Kruch, S. and Chaboche, J.-L., Oxidation Induced Stress Fields in an EB-PVD Thermal Barrier Coating, Surf. Coat. Technol., Vol.157 (2002), pp.103–110.

(12) Schlichting, K.W., Padture, N.P., Jordan, E.H. and Gell, M., Failure Modes in Plasma-Sprayed Thermal Barrier Coatings, Mater. Sci. and Eng., A, Vol.342 (2003), pp.120–130.